Quaternary Geochronology xxx (xxxx) xxx–xxx

Contents lists available at ScienceDirect

Quaternary Geochronology

journal homepage: www.elsevier.com/locate/quageo

Research paper

Single-grain OSL dating of the Middle Palaeolithic site of Galería de las Estatuas, Atapuerca (Burgos, Spain)

Martina Demuro[a,*], Lee J. Arnold[a], Arantza Aranburu[b], Asier Gómez-Olivencia[c,d,e], Juan-Luis Arsuaga[e,f]

[a] School of Physical Sciences, Environment Institute, Institute for Photonics and Advanced Sensing (IPAS), University of Adelaide, North Terrace Campus, 5005 Adelaide, SA, Australia
[b] Departamento Mineralogía y Petrología, Facultad de Ciencia y Tecnología, Universidad del País Vasco, Edificio F3, Barrio Sarriena s/n, 48940 Leioa, Bizkaia, Spain
[c] Departamento de Estratigrafía y Paleontología, Facultad de Ciencia y Tecnología, Euskal Herriko Unibertsitatea, UPV-EHU, Barrio Sarriena s/n, 48940 Leioa, Spain
[d] IKERBASQUE, Basque Foundation for Science, 48013 Bilbao, Spain
[e] Centro Mixto Universidad Complutense-Instituto de Salud Carlos III de Evolución y Comportamiento Humano, Avd. Monforte de Lemos 5, (Pabellón 14), 28029 Madrid, Spain
[f] Departamento de Paleontología, Facultad de Ciencias Geológicas, Universidad Complutense de Madrid, c/ José Antonio Novais, Ciudad Universitaria, 28040 Madrid, Spain

ARTICLE INFO

Keywords:
Single-grain OSL
TT-OSL
Atapuerca
Middle Palaeolithic
Neandertal
Iberia
Spain

ABSTRACT

This study presents single-grain optically stimulated luminescence (OSL) chronologies for the archaeological site of Galería de las Estatuas – the first systematically excavated Middle Palaeolithic site within the karst system of the Sierra de Atapuerca archaeological complex, northern Spain. The single-grain OSL ages are compared with paired single-grain thermally transferred OSL (TT-OSL) dating results for a selection of samples in order to better assess quartz signal bleaching characteristics of endokarstic deposits preserved at Atapuerca. In total, seven luminescence dating samples were collected from four lithostratigraphic units exposed in two excavation pits (GE-I and GE-II). The single-grain OSL equivalent dose (D_e) distributions are characterised by generally low overdispersion (20–30%), suggesting appropriate bleaching at deposition. The resultant single-grain OSL ages reveal that the sediment sequence and archaeological remains excavated in pit GE-I accumulated 80–112 ka, while the upper layers of excavation area GE-II were deposited 70–79 ka. The replicate single-grain TT-OSL ages are in agreement with the OSL chronologies at 2σ for three of the four samples investigated; although in all cases the TT-OSL ages were systematically older than their single-grain counterparts. Apparent TT-OSL residual doses (i.e., TT-OSL D_e values in excess of their corresponding OSL D_e values) of 9–65 Gy were observed for all samples. These excess TT-OSL D_e values are generally low in comparison to the natural dose ranges of TT-OSL dating applications undertaken elsewhere in the Atapuerca karst system. The single-grain TT-OSL and OSL dating comparisons build on daylight bleaching experiments and modern analogue studies performed on other Atapuerca exogeneous infill deposits and suggest reasonable potential for TT-OSL signal resetting down to relatively low levels for at least some sediments preserved in the Atapuerca karstic cavities. The quartz single-grain OSL chronologies obtained in this study place the Middle Palaeolithic sequence of Galería de las Estatuas within marine isotope stage (MIS) 5 and the beginning of MIS 4, and provide firm evidence for human occupation of the Sierra de Atapuerca during a previously unreported time period.

1. Introduction

The extensive karst system of the Sierra de Atapuerca (northern Iberian Plateau, Spain; Fig. 1a) preserves several Early and Middle Pleistocene allochthonous infill sites (e.g., Gran Dolina, Galería complex, Sima del Elefante and Sima de los Huesos), which showcase important palaeoanthropological (*Homo antecessor* and early representatives of the Neandertal lineage; Bermúdez de Castro et al., 1997; Arsuaga et al., 2014), mammal faunal (Rodríguez et al., 2011) and Lower Palaeolithic records (Carbonell et al., 2008; Ollé et al., 2013), as well as extensive Upper Palaeolithic and Neolithic sequences (Carretero et al., 2008; Bañuls-Cardona et al., 2017). More than 30 Middle Palaeolithic open-air sites have additionally been discovered in the vicinity (< 2 km) of the Atapuerca hills and surrounding river

* Corresponding author.
E-mail address: martina.demuro@adelaide.edu.au (M. Demuro).

https://doi.org/10.1016/j.quageo.2018.02.006
Received 4 December 2017; Received in revised form 5 February 2018; Accepted 23 February 2018

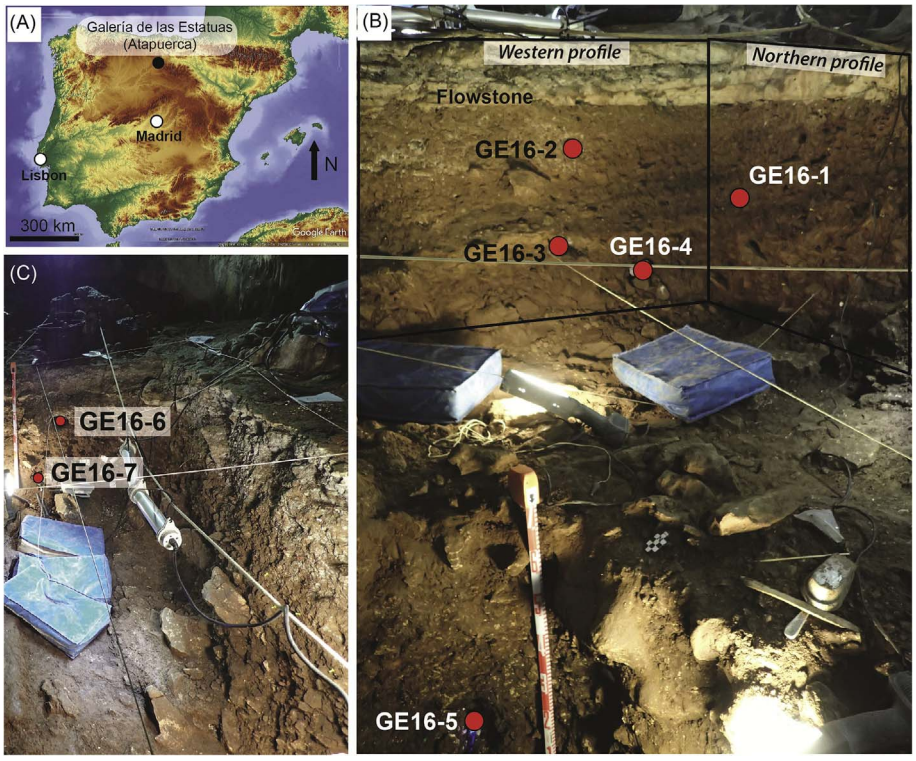

Fig. 1. (A) Map of the Iberian Peninsula showing the location of the Galería de las Estatuas archaeological site (Atapuerca). (B) Photo of excavation pit GE-I showing the profile exposed on the western and northern faces and the position of the five samples collected for luminescence dating. (C) Photo of excavation pit GE-II showing the profile on the southern face and the position of the two luminescence dating samples collected.

valleys (Navazo and Carbonell, 2014), and several of these sites have revealed rich Middle Palaeolithic assemblages (Navazo et al., 2011; Arnold et al., 2013). Until recently, however, equivalent Middle Palaeolithic records have not been reported from within the karst system (Aranburu et al., 2012). In this regard, Galería de las Estatuas represents an important new archaeological sequence within the Sierra de Atapuerca complex. It is the first Middle Palaeolithic site (< 200 ka) to be systematically excavated within the endokarstic infill deposits of Atapuerca, and it is invaluable for providing improved insights into Neandertal occupational histories and subsistence/exploitation strategies in the region (Arsuaga et al., 2017).

The main archaeological and palaeoecological findings at Galería de las Estatuas have been summarised in Arsuaga et al. (2017) and include: (i) a lithic assemblage composed of 499 objects showing clear Mousterian affinities (e.g., centripetal flake cores, side-scrapers, denticulates), with some products displaying characteristic Levallois débitage; (ii) a detailed pollen record revealing, from the base upwards, a change from an open environment and dry/cool climate to a phase of shrub expansion, followed by an incremental increase in wooded species, and a more humid and warmer climate at the top of the sequence; and (iii) an extensive micro- and macro-mammal faunal record, with the latter being dominated by ungulates and displaying abundant evidence of human modification (cut marks and anthropogenic breakage). The only chronological constraint available for this new site is a series of eight radiocarbon (^{14}C) ages obtained on faunal remains from levels LU1 and LU3, which range from 43.5 to > 46.3 ^{14}C ka BP (uncalibrated), and a U-series age of ~14 ka obtained for the base of a stalagmitic crust capping the entire sedimentary sequence (Martínez-Pillado et al., 2014; Arsuaga et al., 2017). All of the ^{14}C ages are close to the analytical limits of the technique; five out of the eight samples yield infinite uncalibrated age ranges, and all eight samples yield non-finite 95.4% calibrated age ranges. Consequently, Arsuaga et al. (2017) cautiously interpreted these ^{14}C results as minimum ages and were only able to suggest that the archaeological accumulation at Galería de las Estatuas is likely of Late Pleistocene age. Given these problems, and the limited stratigraphic coverage of existing age control, there remains a need for a more comprehensive chronological study of the site.

The main aim of this study is to provide the first detailed chronological constraint on the various sediment layers at Galería de las Estatuas using single-grain optically stimulated luminescence (OSL) dating. We also present paired single-grain thermally transferred OSL (TT-OSL) dating comparisons for a subset of samples, with the aim of investigating the applicability of this approach for the Late Pleistocene infill karst deposits at Galería de las Estatuas. The majority of luminescence dating studies undertaken elsewhere on (> 200 ka) sedimentary sequences at Atapuerca have used alternative 'extended-range' luminescence signals with higher dose saturation limits (Berger et al., 2008), including single-grain TT-OSL and post infrared IRSL dating (Demuro et al., 2014; Arnold et al., 2014, 2015; Arnold and Demuro, 2015). However, the relatively slow bleaching characteristics of TT-OSL signals (on the order of days, compared to seconds for the conventional OSL dating signal; Duller and Wintle, 2012; Duval et al., 2017) means that higher residual doses and age overestimation are a potential problem in this setting (Wang et al., 2006; Tsukamoto et al., 2008; Jacobs et al., 2011). An additional aim of this study is therefore to gain insights into TT-OSL signal resetting experienced by some of the younger Atapuerca karstic sediments, via assessments of quartz luminescence signals that bleach at different rates.

2. Site description and luminescence dating samples

The site of Galería de las Estatuas is situated 1020 masl in the uppermost level of the Cueva Mayor–Cueva del Silo karst system (Fig. S1), adjacent to a palaeoentrance that has been sealed by a stalagmitic flowstone. Two test pits (< 2 m-deep), denoted GE-I (9 m^2; ca. 2 m-deep) and GE-II (6 m^2; ca. 1.5 m-deep), have been excavated at this site. These test pits are located c. 18–20 m from the ancient cave entrance (Ortega, 2009). In GE-I, five lithostratigraphic units (LU) have been identified within the sedimentary sequence below the capping flowstone, while in GE-II, which has been less extensively excavated, only two LUs have currently been identified (Arsuaga et al., 2017). Archaeological and palaeontological remains have been recovered from all LUs, although the material recovered from LU1 and LU5 in pit GE-I was relatively scarce. Sedimentological analyses of the LUs from both

excavation pits indicate that the preserved sediment is allochthonous to the karst system (Aranburu et al., 2012; see Supplementary Information for further description of each LU). Transportation of these deposits into the cave interior is thought to have occurred via gravitational mass movement of water-saturated clays (i.e., debris flows), which simultaneously carried various proportions of clasts into the cavity (Arsuaga et al., 2017). The morphology of the gallery, as well as the position of the karstic infill deposits in relation to the cave entrance, suggest that the opening was a shallow ramp that allowed the progressive accumulation of fine-grain sediments and clasts under direct or indirect daylight, and ensured their subsequent transportation 20 m towards the cave interior during discrete runoff events (ramp inclination at the points of excavation is 5–8°). The allochthonous cave infill deposits being dated in this study originate from surface soils immediately surrounding the cave entrance, which contain a significant proportion of wind-blown silts and sands (Berger et al., 2008). Aeolian transportation and continued sub-aerial surface reworking of these sediments is likely to have favoured prolonged exposure to sunlight and full OSL signal resetting prior to being washed into the cave; as borne out by the very low residual D_e value obtained for modern surface sediments collected adjacent to several of the Atapuerca endokarst entrances (-0.03 ± 0.04 to 0.18 ± 0.07 Gy; see Arnold et al., in press). The relatively close proximity of the studied excavation pits to the original cave entrance is also thought to have favoured minimal sediment transportation residence times within the cavity prior to final deposition.

In total, seven luminescence dating samples were collected from the karstic infill deposits of Galería de las Estatuas as part of the present study: five samples were obtained from excavation pit GE-I (Fig. 1b) and two samples were taken from pit GE-II (Fig. 1c).

3. Luminescence dating methods

3.1. Instrumentation, dose rates and equivalent dose (D_e) estimation

Full details of the luminescence dating procedures employed in this study, including sample preparation, instrumentation, dose rate estimation, single-grain rejection criteria, and D_e measurement procedures, are provided in the Supplementary Information. Single-grain OSL dating was undertaken on all seven samples, while additional single-grain TT-OSL measurements were made on selected samples (GE16-1, GE16-4, GE16-6 and GE16-7). Environmental dose rates (Table S1) have been determined using a combination of in situ gamma spectrometry and low-level beta counting. Cosmic-ray dose rates have been calculated using the approach described in Prescott and Hutton (1994).

Single-grain OSL and TT-OSL D_e measurements were made using the single-aliquot regenerative-dose (SAR) protocols described in Murray and Wintle (2000) and Stevens et al. (2009), respectively, which were modified to enable measurements of individual grains (e.g., Arnold et al., 2016; Demuro et al., 2014; Table S3). Single-grain dose recovery tests performed on both the OSL and TT-OSL signals support the suitability of the SAR protocols for dating these samples (corresponding dose recovery ratios = 0.98 ± 0.03 and 1.12 ± 0.14; see Supplementary Information, Fig. S2 and Table S4).

4. Results

4.1. Single-grain OSL signal characteristics and D_e estimates

Approximately 30–70% of the measured grains produced detectable OSL signals, with the brightest grains (1–3%) having 100-10,000 net counts/Gy in the first 0.09 s stimulation (Fig. 2a). The measured OSL signals were also fast-decaying and were generally depleted by > 90% within the first 0.18 s of stimulation. After applying the SAR rejection criteria, 4–9% of the measured grains were considered suitable for D_e estimation (Table S5). An example of a sensitivity-corrected dose-response and OSL decay curve for a moderately bright grain that passed the rejection criteria is shown in Fig. 2b.

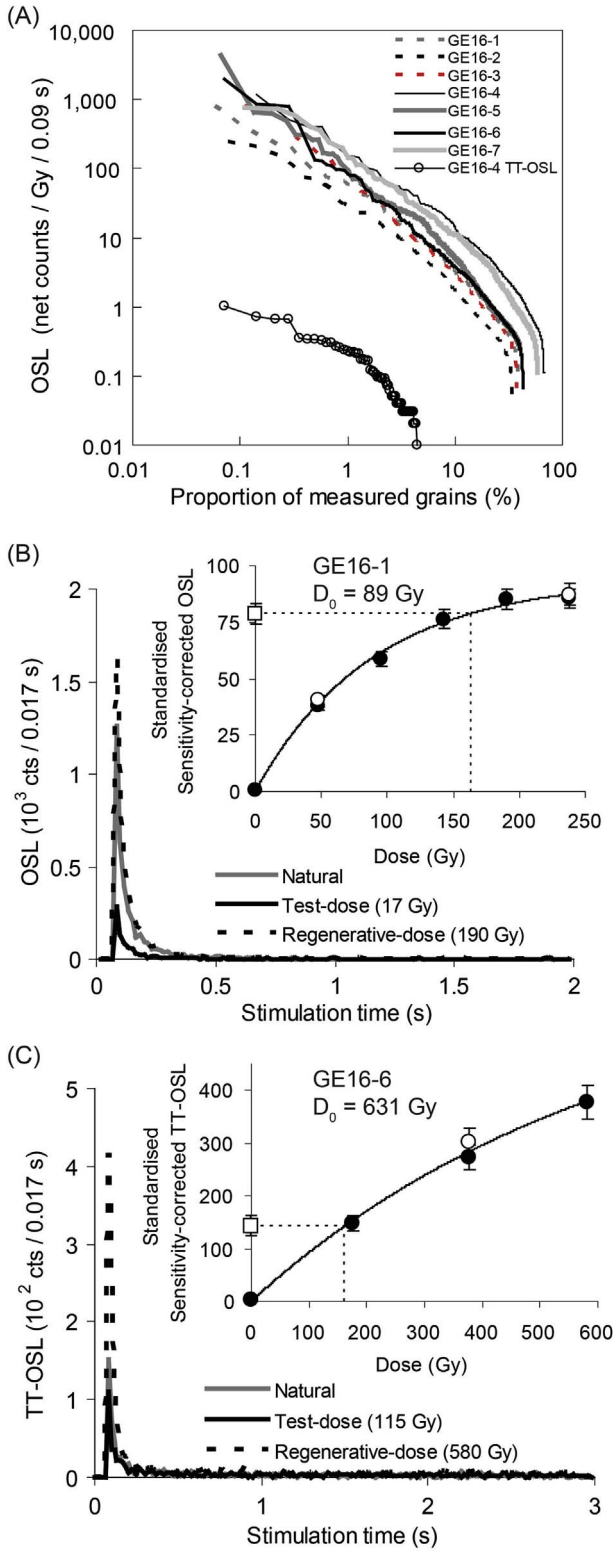

Fig. 2. (A) OSL signal brightness plot showing absolute net intensities expressed as counts/Gy/0.09 s. The data shown are for single-grain OSL measurements made using the 212–250 μm quartz fraction for all samples except GE16-4, for which the 250–300 μm fraction was used; also shown is the single-grain TT-OSL signal brightness plot for the 250–300 μm fraction of sample GE16-4 (1 grain per hole). Examples of (B) OSL and (C) TT-OSL decay curves and sensitivity-corrected dose-response curves (inset) for two grains from samples GE16-1 and GE16-6.

The single-grain OSL D_e distributions display relatively low scatter,

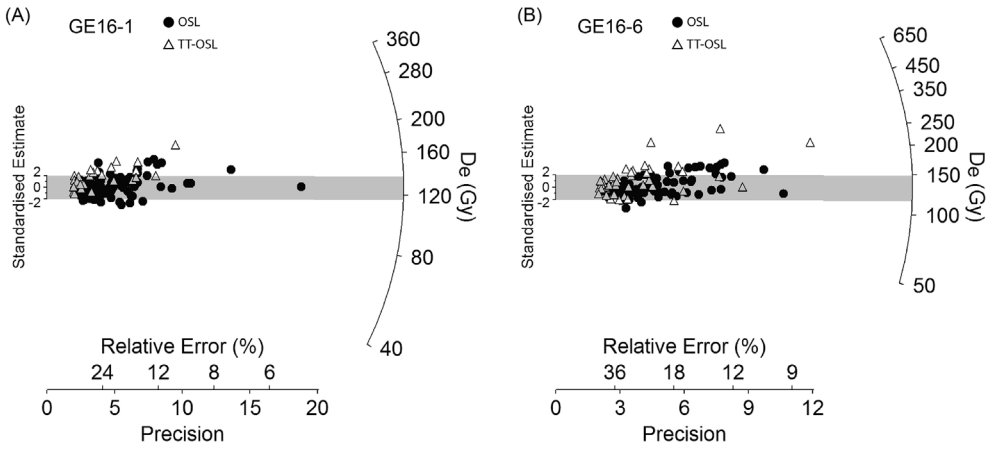

Fig. 3. Radial plots showing the paired single-grain OSL and single-grain TT-OSL D_e distributions obtained for samples (A) GE16-1 and (B) GE16-6 (D_e errors are shown at 1σ). The grey band is centred on the central age model D_e obtained for the OSL dataset.

with six out of the seven samples producing overdispersion values of 20–26% and one sample (GE16-7) producing a slightly higher, albeit consistent, overdispersion of 30 ± 4% (Fig. 3 and Fig. S4; Table 1). None of the samples are considered to be significantly positively skewed according to the criterion outlined by Arnold and Roberts (2009). The overdispersion values of these karstic infill samples are also in agreement at 2σ with what is typically observed for well-bleached samples (~20%; Arnold and Roberts, 2009) and, with the exception of GE16-7, they are consistent at 2σ with the overdispersion value obtained in the dose-recovery test (10 ± 5%). Representative single-grain OSL burial dose estimates have therefore been calculated using the central age model (CAM) of Galbraith et al. (1999). The single-grain CAM D_e values obtained for the Galería de las Estatuas samples range between 85 and 145 Gy (Table 1).

The reliability of the single-grain OSL D_e estimates, as well as their usefulness for undertaking comparative TT-OSL bleaching assessments, will partly depend on whether the accepted grain populations have sufficiently high dose saturation limits to ensure finite D_e estimation over the true natural burial dose ranges of interest (particularly as the measured D_e values typically exceed 100 Gy). To examine whether the single-grain OSL CAM D_e values have been compromised by dose saturation, we analysed the characteristic saturation dose (D_0) value for each accepted grain. The weighted mean (CAM) D_0 value for the combined Galería de las Estatuas sample dataset, calculated from all grains (n = 521), is 87 ± 1 Gy (Fig. S5). The majority of accepted grains (~90%) produced D_0 values in the range of 40–160 Gy, with the remaining grains (~10%) having D_0 values of > 160 Gy. In general, these D_0 values are high enough to enable finite D_e determination over the burial dose ranges of these samples (50–250 Gy); hence we do not consider that the single-grain OSL ages have been negatively affected by dose saturation. To explore this issue further, we applied the 2 × D_0 acceptance threshold criterion outlined by Demuro et al. (2015), which ensures that only grains with 2 × D_0 values higher than a specific burial dose are accepted for final D_e estimation. This additional quality assurance criterion is designed to eliminate grains that produce unrealistically low D_e values purely as a result of insufficient dose saturation limits, thus avoiding potential age underestimation arising from inherently unsuitable grains. Progressively higher 2 × D_0 thresholds of 140–260 Gy (increasing in 40 Gy increments) were applied to all the samples, and the effects on weighted mean D_e were examined after taking into consideration associated 2σ uncertainty ranges (see details in Arnold et al., 2016). For all seven samples, it was found that selecting grains with progressively higher D_0 values did not result in significantly higher CAM D_e values (Fig. S6). Instead, both the CAM D_e and overdispersion (data not shown) remained within 2σ of the original values. Although a slight decrease in D_e is observed in samples GE16-4 and GE16-5 after a 2 × D_0 threshold of 220 Gy is applied, this trend is not deemed statistically significant since the resulting ages do not deviate beyond the 1σ ranges of the original values. These results indicate that the original single-grain OSL D_e values (and ages) calculated using all accepted grains were not adversely affected by OSL dose saturation.

4.2. Single-grain OSL ages

The single-grain OSL ages obtained for excavation pit GE-I are stratigraphically consistent and range between ~112 ka and ~80 ka (Table 1). These ages indicate that the sequence at GE-I was deposited during marine isotope stage (MIS) 5. The sedimentary sequence in excavation pit GE-II (upper units) has a similar, albeit slightly younger, chronology, which extends from the end of MIS 5 to the beginning of MIS 4; stratigraphically consistent ages of 79 ± 5 ka (GE16-7) and 70 ± 5 ka (GE16-6) were obtained for LU2 and LU1, respectively. These single-grain OSL dating results suggest that the two sedimentary sequences excavated at Galería de las Estatuas potentially cover the same time period (when considering their 2σ age ranges). The upper half of LU2 and LU1 in excavation pit GE-I are therefore likely correlative with LU2 from excavation pit GE-II.

4.3. Single-grain TT-OSL dating results

The majority of measured grains (60–80%) did not produce detectable TT-OSL signals (Table S6). Grains that did produce TT-OSL signals were generally very dim (e.g., the brightest 1% of grains produced 0.5–1 net counts/Gy/0.09 s; Fig. 2a), with only 1–5% of measured grains being accepted for final D_e estimation (Table S6). An example of a representative TT-OSL dose response and decay curve for an accepted grain is shown in Fig. 2c. The single-grain TT-OSL D_e distributions of samples GE16-1, GE16-4 and GE16-7 were generally less scattered than their OSL counterparts (overdispersion values were 18–21%), with only sample GE16-6 having a higher overdispersion (45%) (Table 1; Fig. S7). All four samples produced CAM D_e values that were higher (by 9–65 Gy) than their corresponding single-grain OSL CAM D_e values (after correcting for dose rate differences related to the different grain sizes being measured). However, three of the four samples (GE16-4, GE16-6 and GE16-7) produced final single-grain TT-OSL ages in agreement with their paired single-grain OSL ages at 2σ (Table 1).

The TT-OSL age of GE16-7 (84 ± 7 ka) was in closest agreement with its OSL counterpart (79 ± 5 ka), and this sample may be regarded as having experienced adequate TT-OSL signal bleaching at deposition. The low number of D_e values obtained for GE16-4 (n = 14; Table 1), and the large uncertainty associated with the final age estimate,

Table 1
Single-grain OSL ages for Galería de las Estatuas. Also shown are the comparative single-grain TT-OSL ages obtained for four of the samples. Ages shown in bold have been used to derive the final chronologies for each sample (see main text for further discussions).

Sample	LU [a]	Single-grain OSL							Single-grain TT-OSL						
		Grain size (μm) [b]	Total dose rate (Gy/ka)	Accepted/ measured grains [c]	Overdispersion (%) [d]	Age Model [d]	D_e (Gy) [f]	Age (ka) [f,g]	Grain size (μm) [b]	Total dose rate (Gy/ka)	Accepted/ measured grains [c]	Overdispersion (%) [d]	Age Model [d,e]	D_e (Gy) [f]	Age (ka) [f,g]
Excavation GE-II															
GE16-6	1	212–250	1.88 ± 0.09	80/1400	26 ± 4	CAM	132 ± 5	**70 ± 5**	90–125	1.97 ± 0.09	43/1400	45 ± 7	CAM	169 ± 14	86 ± 8
													MAM-3	*115 ± 15*	*58 ± 8*
													MAM-4	*110 ± 21*	*56 ± 11*
GE16-7	2	212–250	1.82 ± 0.09	79/900	30 ± 4	CAM	145 ± 6	**79 ± 5**	90–125	1.91 ± 0.10	35/700	21 ± 8	CAM	161 ± 10	84 ± 7
Excavation GE-I															
GE16-2	1	212–250	1.22 ± 0.06	52/1300	20 ± 4	CAM	97 ± 4	**80 ± 5**							
GE16-1	2	212–250	1.53 ± 0.08	94/1700	26 ± 3	CAM	127 ± 5	**83 ± 5**	90–125	1.61 ± 0.08	28/1100	20 ± 6	CAM	198 ± 13	123 ± 10
GE16-3	2	212–250	0.75 ± 0.04	53/900	21 ± 4	CAM	85 ± 4	**113 ± 8**							
GE16-4	3	250–300	1.04 ± 0.06	62/700	26 ± 4	CAM	111 ± 5	**107 ± 8**	250–300	1.04 ± 0.06	14/1400	18 ± 12	CAM	131 ± 13	126 ± 14
GE16-5	4	212–250	1.13 ± 0.06	101/1500	22 ± 3	CAM	126 ± 4	**112 ± 7**							

[a] LU = Lithostratigraphic unit.

[b] Measurements were made on single-grain discs containing 300 × 300 μm grain-hole positions. The number of grains contained in each grain-hole position is expected to be as follows: 90–125 μm grains = 18 grains per hole; 212–250 μm grains = 1–2 grains per hole; 250–300 μm grains = 1 grains per hole (Arnold et al., 2012).

[c] Number of D_e measurements that passed the SAR rejection criteria/total number of grains or multi-grain aliquots analysed.

[d] CAM = central age model; MAM-3 = three-parameter minimum model; MAM-4 = four-parameter minimum age model (Galbraith et al., 1999); Overdispersion parameter has been calculated using the CAM.

[e] MAM-3 and MAM-4 D_e estimates have been calculated after adding, in quadrature, a relative error of 15% to each individual D_e measurement error to approximate underlying dose overdispersion observed in typical sedimentary samples (Arnold and Roberts, 2009; Arnold et al., in press).

[f] Mean ± total uncertainty (68% confidence interval), calculated as the quadratic sum of the random and systematic uncertainties.

[g] Total uncertainty includes a systematic component of ± 2% associated with laboratory beta-source calibration.

potentially complicate the interpretations of TT-OSL bleaching adequacy for this sample. The TT-OSL and OSL ages of this sample are in agreement at 2σ but additional single-grain TT-OSL measurements would be needed to confirm its TT-OSL bleaching history. For sample GE16-6, the CAM TT-OSL age (86 ± 8 ka) is within 2σ of the OSL age (70 ± 5 ka) but the large overdispersion obtained for the TT-OSL dataset (45 ± 7%) (Table 1) may indicate additional, extrinsic D_e scatter related to minor populations of partially bleached grains (Fig. 3). Application of the 3-parameter and 4-parameter minimum age models (MAM-3 and MAM-4; Galbraith et al., 1999) to this TT-OSL D_e dataset produced ages that were systematically younger than (though within 2σ of) the single-grain OSL age of GE16-6 (in italics Table 1). Sample GE16-1 displays the highest offset between its replicate single-grain TT-OSL and OSL ages. Although the TT-OSL D_e dataset for this sample has a low overdispersion of 20 ± 6%, which may indicate full signal resetting, the TT-OSL CAM D_e is ~50% higher than its OSL counterpart, and the resulting TT-OSL age (123 ± 10 ka) overestimates the OSL age (83 ± 5 ka) beyond its 2σ uncertainty ranges. It may be worth noting that the single-grain TT-OSL dose recovery test yielded a measured-to-given dose ratio that was systematically in excess of unity by ~12% (albeit consistent with the given dose at 2σ). The higher TT-OSL age for sample GE16-1 may therefore partly originate from intrinsic D_e scatter related to the chosen SAR measurement protocol.

5. Discussion and conclusion

The single-grain TT-OSL and OSL dating comparisons undertaken in this study build on daylight bleaching experiments and modern analogue studies performed elsewhere on Atapuerca exogeneous infill deposits (Demuro et al., 2015; Arnold et al., in press), and suggest reasonable potential for TT-OSL signal resetting down to relatively low levels for some sediments preserved in the Atapuerca karstic cavities. All four samples contained large populations of grains with seemingly well-bleached TT-OSL signals, indicating prolonged (> 6 weeks; Demuro et al., 2015, Arnold et al., in press) exposure to sunlight prior to burial within the cave. The single-grain TT-OSL ages are in agreement with the replicate OSL chronologies at 2σ for three of the four samples investigated; although in all cases the TT-OSL ages were systematically older than their single-grain counterparts. Mean TT-OSL residual doses (calculated as the difference between paired OSL and TT-OSL CAM D_e values) varied widely for the four samples, ranging between ~9 and ~65 Gy after correcting for grain-size dosimetric effects. These results suggest that it may be unsuitable to generalise about TT-OSL dating adequacy for allochthonous cave infill deposits without undertaking site-specific assessments. As our dating comparisons demonstrate, a useful approach for assessing TT-OSL bleaching adequacy involves simultaneously applying a suite of luminescence signals that are optically reset at different rates (i.e., OSL, pIR-IR), particularly when reliable independent age control is unavailable (e.g., Demuro et al., 2014, 2015; Hamm et al., 2016; Jacobs et al., 2017; Arnold et al., in press). In general, the mean TT-OSL residual doses observed at Galería de las Estatuas are relatively low in comparison to the natural dose ranges of TT-OSL dating applications undertaken elsewhere in the Atapuerca karst system (either due to their high environmental dose rates or older depositional ages). Residual D_e values on the order of several Gy or tens of Gy are likely to be well within the existing 2σ TT-OSL age uncertainties for most Middle or Early Pleistocene samples, and therefore are unlikely to have major effects on extended-range TT-OSL dating reliability.

Our single-grain OSL ages for Galería de las Estatuas place the sedimentary sequence of excavation pit GE-I (Fig. 4) within MIS 5 (80 ± 5 ka to 112 ± 7 ka) and the sequence at excavation pit GE-II (upper section) within late MIS 5 and early MIS 4 (70 ± 5 ka to 79 ± 5 ka); though the chronologies of GE-I and GE-II are statistically indistinguishable at 2σ. As expected, these luminescence chronologies are older than the preliminary ^{14}C ages reported for the site (> 45 cal ka BP – > 49.5 cal ka BP; Table S7), confirming the original interpretation of Arsuaga et al. (2017) that their ^{14}C results should be considered as minimum age estimates. Our ages for GE-I and GE-II are stratigraphically consistent and suggest that the two sequences excavated at Galería de las Estatuas are likely temporally correlative, although further dating at the base of pit GE-II is required to determine the lower chronological range of this sequence. It is worth noting that the age of sample GE16-3 (113 ± 8 ka), which was collected from a localised sub-layer at the base of LU2, is in closer agreement with the age obtained for the underlying level (LU3) (107 ± 8 ka; GE16-4), rather than the age obtained for the upper section of LU2 (83 ± 5 ka; GE16-1). Further dating efforts and more detailed sedimentological studies of this sub-layer may be necessary to ascertain its exact chronostratigraphic relationship with LU2 and LU3. Together, the single-grain OSL ages obtained for GE-I indicate that the pollen-based climatic reconstructions at this excavation pit – which show a change from an open environment and dry/cool conditions (lower LU3 and LU4) towards a phase of shrub expansion (upper LU3) and a more humid and warmer climate, followed by an increase in wooded species (LU2) at the top of the sequence – may be associated with MIS 5.4 (LU3-4) and MIS 5.1 (LU2), respectively (Lisiecki and Raymo, 2005, Fig. 4). Although it is difficult to make more precise correlations between the climatic reconstructions at Galería de las Estatuas and global $\delta^{18}O$ isotope stages, both the pollen record and the chronologies obtained suggest that LU4 was deposited post-MIS 5.5 (Fig. 4).

Galería de las Estatuas is the first archaeological site within the Sierra de Atapuerca karst system to be dated to MIS 4/5. Within a regional context, several other Middle Palaeolithic and Neandertal sites from the surrounding valleys of the northern Iberian meseta region could be considered to be chronologically equivalent to Galería de las Estatuas (Table S7). The open-air sequences of Hotel California and Hundidero, located in the vicinity of the Atapuerca hills, have chronologies of 70–45 ka based on single-grain OSL and TL dating of sedimentary grains, respectively (Arnold et al., 2013; Navazo et al., 2011), and may be partially correlative with, albeit slightly younger than, Galería de las Estatuas. The Neandertal cave site of Valdegoba located a short (< 30 km) distance from Atapeurca may also have a similar chronology. The sequence is capped by a speleothem that has been U-series dated to < 73.2 ± 5 ka (Quam et al., 2001). An additional AMS ^{14}C ultrafiltration age of 48.4 ± 3.3 ka (uncalibrated) has been obtained from the human-bearing layers of Valdegoba (Dalén et al., 2012), which may be regarded as a minimum age due to its antiquity. La Ermita, another nearby cave site (Díez et al., 2008), could also be dated to MIS 5. This site has a ^{14}C age of 32.1–34.2 ka cal BP (Díez et al., 2008), but a U-series age of 95–102 ka has been recently reported for a speleothem capping the sediment sequence (Sánchez Yustos and Diez Martín, 2016). Other sites with similar chronologies on the Iberian plateau include San Quirce (73 ± 10 ka; Terradillos-Bernal et al., 2017) and Cueva del Camino, near Madrid (74–140 ka; Arsuaga et al., 2012). While in the Cantabrian Range to the north, the site of El Castillo also covers a similar time span (level 23 dated to ~90 ka; Bischoff et al., 1992). However, further dating studies are required at some of these sites to fully elucidate the Late Pleistocene Neandertal occupation histories in the region, especially in cases where ^{14}C dating appear to have reached its upper limits (Table S7). The chronological results obtained in the present study for Galería de las Estatuas indicate that single-grain OSL dating has the potential to make important contributions towards this effort.

Acknowledgements

We dedicate this paper to Glen Berger who worked closely with the excavation and research teams at Atapuerca over many years. Financial support for this research was provided by Australian Research Council (ARC) Discovery Early Career Researcher Award DE160100743 and Future Fellowship project FT130100195. We would like to

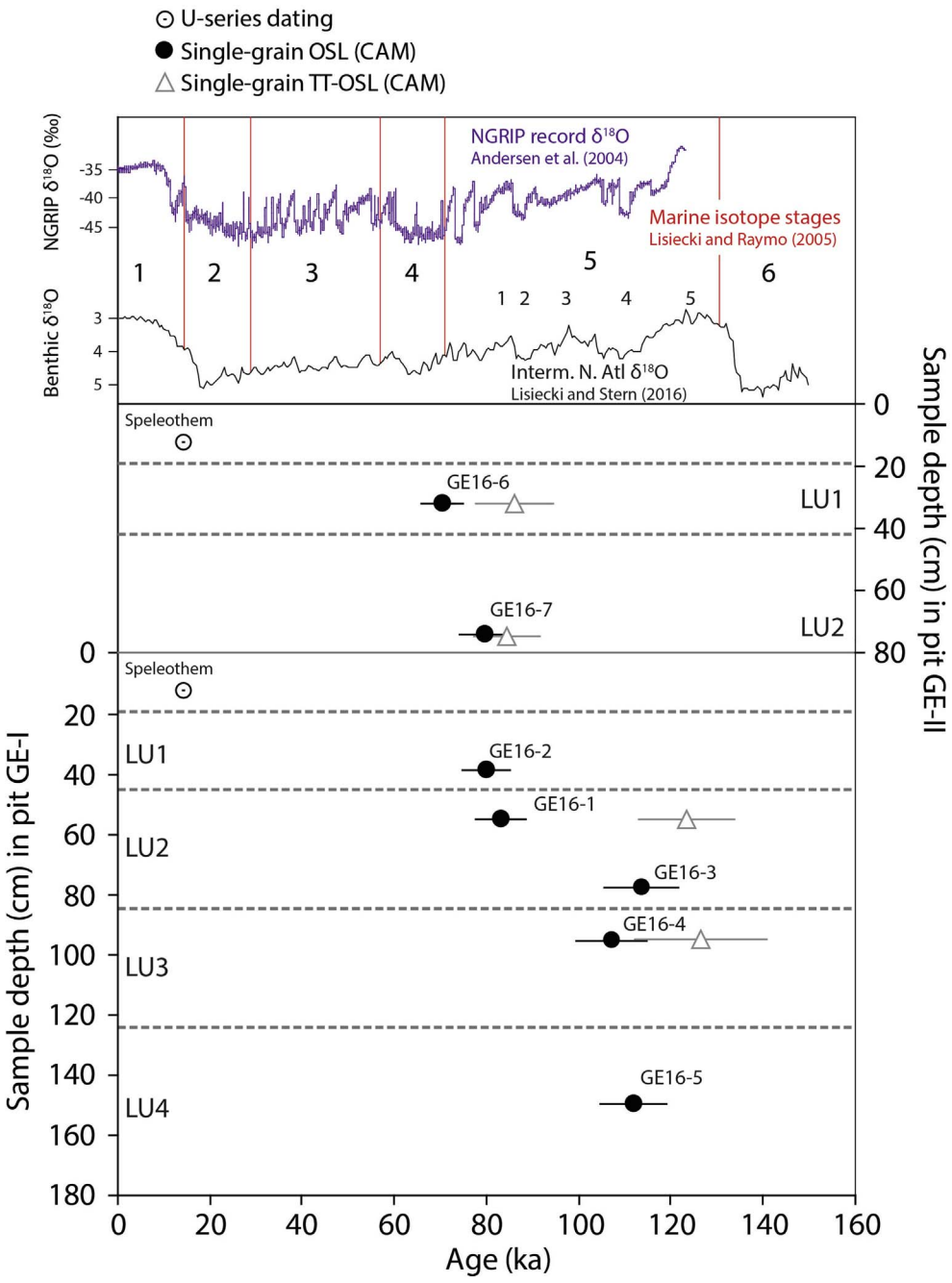

Fig. 4. Single-grain OSL ages (and associated 1σ errors) for the seven luminescence samples collected from Galería de las Estatuas (black circles), plotted against and the $\delta^{18}O$ isotope curves for the last glacial cycle (NGRIP and Intermediate North Atlantic records; Andersen et al., 2004; Lisiecki and Stern, 2016). The ages obtained for each excavation pit are shown on separate panels (GE-I in lower panel; GE-II in upper panel) because the lithostratigraphic unit (LU) numbering systems have been assigned independently for each excavated sequence (Arsuaga et al., 2017). Also shown are the single-grain TT-OSL ages obtained using the central age model (CAM) (white triangles). The continuous capping speleothem extends across both excavation pits, and its age (white circle) is based on previously published data (Martínez-Pillado et al., 2014). The grey hashed lines indicate tentative (spatially averaged) positions of the LU boundaries.

acknowledge the entire GE excavation and research team, and especially the people that helped during sample collection. Fieldwork at Atapuerca was funded by the Junta de Castilla y León and Fundación Atapuerca. The study was supported by the Spanish Ministerio de Ciencia y Tecnología (Projects: CGL2012-38434-C03-01, CGL-2015-65387-C3-2-P) (MINECO/FEDER).

Appendix A. Supplementary data

Supplementary data related to this article can be found at http://dx.doi.org/10.1016/j.quageo.2018.02.006.

References

Andersen, K.K., Azuma, N., Barnola, J.-M., Bigler, M., Biscaye, P., Caillon, N., Chappellaz, J., Clausen, H.B., Dahl-Jensen, D., Fischer, H., Flückiger, J., Fritzsche, D., Fujii, Y., Goto-Azuma, K., Grønvold, K., Gundestrup, N.S., Hansson, M., Huber, C., Hvidberg, C.S., Johnsen, S.J., Jonsell, U., Jouze, J., Kipfstuh, S., Landais, A., Leuenberger, M., Lorrain, R., Masson-Delmotte, V., Miller, H., Motoyama, H., Narita, H., Popp, T., Rasmussen, S.O., Raynaud, D., Rothlisberger, R., Ruth, U., Samyn, D., Schwander, J., Shoji, H., Siggard-Andersen, M.-L., Steffensen, J.P., Stocker, T., Sveinbjörnsdóttir, A.E., Svensson, A., Takata, M., Tison, J.-L., Thorsteinsson, Th, Watanabe, O., Wilhelms, F., White, J.W.C., 2004. High-resolution record of Northern hemisphere climate extending into the last interglacial period. Nature 431, 147–151.

Aranburu, A., Martínez-Pillado, V., Arsuaga, J.L., Alcázar de Velasco, A., et al., 2012. La variabilidad de los rellenos endokársticos de la Galería de Estatuas (Atapuerca, Burgos) y su caracterización paleoambiental. In: González-Díez, A. (Ed.), Avances de la Geomorfología en España 2010-2012. Actas de la XII Reunión Nacional de Geomorfología. Santander, 17–20 September 2012.

Arnold, L.J., Roberts, R.G., 2009. Stochastic modelling of multi-grain equivalent dose (D_e) distributions: implications for OSL dating of sediment mixtures. Quat. Geochronol. 4, 204–230.

Arnold, L.J., Demuro, M., Navazo Ruiz, M., 2012. Empirical insights into multi-grain averaging effects from 'pseudo' single-grain OSL measurements. Radiat. Meas. 47, 652–658.

Arnold, L.J., Demuro, M., Navazo Ruiz, M., Benito-Calvo, A., Pérez-González, A., 2013. OSL dating of the Middle Palaeolithic Hotel California site, Sierra de Atapuerca, north-central Spain. Boreas 42, 285–305.

Arnold, L.J., Demuro, M., Parés, J.M., Arsuaga, J.L., Aranburu, A., Bermúdez de Castro, J.M., Carbonell, E., 2014. Luminescence dating and palaeomagnetic age constraint on hominins from Sima de los Huesos, Atapuerca, Spain. J. Hum. Evol. 67, 85–107.

Arnold, L.J., Demuro, M., Parés, J.M., Pérez-González, A., Arsuaga, J.L., Bermúdez de Castro, J.M., Carbonell, E., 2015. Evaluating the suitability of extended-range luminescence dating techniques over Early and Middle Pleistocene timescales: published datasets and case studies from Atapuerca, Spain. Quat. Int. 389, 167–190.

Arnold, L.J., Demuro, M., 2015. Insights into TT-OSL signal stability from single-grain analyses of known-age deposits at Atapuerca, Spain. Quat. Geochronol. 30, 472–478.

Arnold, L.J., Duval, M., Demuro, M., Spooner, N.A., Santonja, M., Pérez-González, A., 2016. OSL dating of individual quartz 'supergrains' from the Ancient Middle Palaeolithic site of Cuesta de la Bajada, Spain. Quat. Geochronol. 36, 78–101.

Arnold, L.J., Demuro, M., Spooner, N.A., Prideaux, G.J., McDowell, M.C., Camens, A.B., Reed, E.H., Parés, J.M., Arsuaga, J.L., Bermúdez de Castro, J.M., Carbonell, E., 2018;al., in press. Single-grain TT-OSL bleaching characteristics: insights from modern analogues and OSL dating comparisons. Quat. Geochronol. http://dx.doi.org/10.1016/j.quageo.2018.01.004. in press.

Arsuaga, J.L., Baquedano, E., Pérez-González, A., Sala, N., Quam, R.M., Rodríguez, L., García, R., García, N., Alvarez-Lao, D.J., Laplana, C., Huguet, R., Sevilla, P., Maldonado, E., Blain, H.-A., Ruiz-Zapata, M.B., Sala, P., Gil-García, J., Uzquiano, P., Pantoja, A., Márquez, B., 2012. Understanding the ancient habitats of the last interglacial (late MIS 5) Neanderthals of central Iberia: paleoenvironmental and taphonomic evidence from the Cueva del Camino (Spain) site. Quat. Int. 275, 55–75.

Arsuaga, J.L., Martínez, I., Arnold, L.J., Aranburu, A., Gracia-Téllez, A., Sharp, W.D., Quam, R.M., Falguères, C., Pantoja-Pérez, A., Bischoff, J., Poza-Rey, E., Parés, J.M., Carretero, J.M., Demuro, M., Lorenzo, C., Sala, N., Martinón-Torres, M., García, N., Alcázar de Velasco, A., Cuenca-Bescós, G., Gómez-Olivencia, A., Moreno, D., Pablos, A., Shen, C.-C., Rodríguez, L., Ortega, A.I., García, R., Bonmatí, A., Bermúdez de Castro, J.M., Carbonell, E., 2014. Neandertal roots: cranial and chronological evidence from Sima de los Huesos. Science 344, 1358–1363.

Arsuaga, J.L., Gómez-Olivencia, A., Sala, N., Martínez-Pillado, V., Pablos, A., Bonmatí, A., Pantoja-Pérez, A., Lira-Garrido, J., Alcázar de Velasco, A., Ortega, A.I., Cuenca-Bescós, G., García, N., Aranburu, A., Ruiz-Zapata, B., Gil-García, M.J., Rodríguez-Alvarez, X.P., Ollé, A., Mosquera, M., 2017. Evidence of paleoecological changes and Mousterian occupations at the Galeria de las Estatuas site, Sierra de Atapuerca, norther Iberian plateau, Spain. Quat. Res. 88, 345–367.

Bañuls-Cardona, S., López-García, J.M., Morales Hidalgo, J.I., Cuenca-Bescós, G., Vergès, J.M., 2017. Lateglacial to Late Holocene palaeoclimatic and palaeoenvironmental reconstruction of El Mirador cave (Sierra de Atapuerca, Burgos, Spain) using the small-mammal assemblages. Palaeogeogr. Palaeoclimatol. Palaeoecol. 471, 71–81.

Berger, G.W., Pérez-González, A., Carbonell, E., Arsuaga, J.L., Bermúdez de Castro, J.-M., Ku, T.-L., 2008. Luminescence chronology of cave sediments at the Atapuerca paleoanthropological site, Spain. J. Hum. Evol. 55, 300–311.

Bermúdez de Castro, J.M., Arsuaga, J.L., Carbonell, E., Rosas, A., Martínez, I., Mosquera, M., 1997. A hominid from the Lower Pleistocene of Atapuerca, Spain: possible ancestor to neandertals and modern humans. Science 276, 1392–1395.

Bischoff, J.L., Garcia, J.F., Straus, G., 1992. Uranium-series isochron dating at El Castillo cave (cantabria, Spain): the “Acheulean”/“Mousterian” question. J. Archaeol. Sci. 19, 49–92.

Carbonell, E., Bermúdez de Castro, J.M., Parés, J.M., Pérez-González, A., Ollé, A., Mosquera, M., Cuenca-Bescós, G., García, N., Granger, D.E., Huguet, R., van der Made, J., Martinón-Torres, M., Rodríguez, X.P., Rosas, A., Sala, R., Stock, G.M., Vallverdu, J., Vergés, J.M., Allué, E., Benito, A., Burjachs, F., Cáceres, I., Canals, A., Díez, J.C., Lozano, M., Mateos, A., Navazo, M., Rodríguez, J., Rosell, J., Arsuaga, J.L., 2008. The first hominin of Europe. Nature 452, 465–469.

Carretero, J.M., Ortega, J.M., Juez, A.I., Pérez-González, A., Arsuaga, J.L., Pérez-Martínez, R., Ortega, M.C., 2008. A Late Pleistocene-Early Holocene archaeological sequence of Portalón de Cueva Mayor (Sierra de Atapuerca, Burgos, Spain). Munibe (Antropologia - Arkeologia) 59, 67–80.

Dalén, L., Orlando, L., Shapiro, B., Brandström-Durling, M., Quam, R., Thomas, M., Gilbert, P., Díez Fernández-Lomana, J.C., Willerslev, E., Arsuaga, J.L., Gotherström, A., 2012. Partial genetic turnover in Neanderthals: continuity in the east and population replacement in the west. Mol. Biol. Evol. 29, 1893–1897.

Demuro, M., Arnold, L.J., Parés, J.M., Pérez-González, A., Ortega, A.I., Arsuaga, J.L., Bermúdez de Castro, J.M., Carbonell, E., 2014. New luminescence ages for the Galería Complex archaeological site: resolving chronological uncertainties on the Acheulean record of the Sierra de Atapuerca, northern Spain. PLoS One 9, e110169.

Demuro, M., Arnold, L.J., Parés, J.M., Sala, R., 2015. Extended-range luminescence chronologies suggest potentially complex bone accumulation histories at the Early-to-Middle Pleistocene palaeontological site of Huéscar-1 (Guadix-Baza basin, Spain). Quat. Int. 389, 191–212.

Díez, C., Alonso, R., Bengoechea, A., Colina, A., Jordá, J.F., Navazo, M., Ortiz, J.E., Pérez, S., Torres, T., 2008. El Paleolítico Medio en el valle del Arlanza (Burgos), los sitios de La Ermita, Millán y La Mina. Quaternario Geo-morfolgía 22, 135–157.

Duval, M., Arnold, L., Guilarte, V., Demuro, M., Santonja, M., Pérez-Gonzalez, A., 2017. Electron Spin Resonance dating of optically bleached quartz grains from the Middle Palaeolithic site of Cuesta de la Bajada (Spain) using the multiple centres approach. Quat. Geochronol. 37, 82–96.

Duller, G.A.T., Wintle, A.G., 2012. A review of the thermally transferred optically stimulated luminescence signal from quartz for dating sediments. Quat. Geochronol. 7, 6–20.

Galbraith, R.F., Roberts, R.G., Laslett, G.M., Yoshida, H., Olley, J.M., 1999. Optical dating of single and multiple grains of quartz from Jinmium rock shelter, northern Australia: Part I, experimental design and statistical models. Archaeometry 41, 339–364.

Hamm, G., Mitchell, P., Arnold, L.J., Prideaux, G.J., Questiaux, D., Spooner, N.A., Levchenko, V.A., Foley, E.C., Worthy, T.H., Stephenson, B., Coulthard, V., Coulthard, C., Wilton, S., Johnston, D., 2016. Cultural innovation and megafauna interaction in the early settlement of arid Australia. Nature 539, 280–283.

Jacobs, Z., Roberts, R.G., Lachlan, T.J., Karkanas, P., Marean, C.W., Roberts, D.L., 2011. Development of the SAR TT-OSL procedure for dating Middle Pleistocene dune and shallow marine deposits along the southern Cape coast of South Africa. Quat. Geochronol. 6, 491–513.

Jacobs, Z., Li, B., Farr, L., Hill, E., Hunt, C., Jones, S., Rabett, R., Reynolds, T., Roberts, R.G., Simpson, D., Barker, G., 2017. The chronostratigraphy of the Haua Fteah cave (Cyrenaica, northeast Libya) — optical dating of early human occupation during Marine Isotope Stages 4, 5 and 6. J. Hum. Evol. 105, 69–88.

Lisiecki, L.E., Raymo, M.E., 2005. A Pliocene-Pleistocene stack of 57 globally distributed benthic δ18O records. Paleoceanography 20 PA 1003.

Lisiecki, L.E., Stern, J.V., 2016. Regional and global benthic $\delta^{18}O$ stacks for the last glacial cycle. Paleoceanography 31, 1364–1394.

Martínez-Pillado, V., Aranburu, A., Arsuaga, J.L., Ruiz-Zapata, B., Gil-García, M.J., Stoll, H., Yusta, I., Iriarte, E., Carretero, J.M., Edwards, R.L., Cheng, H., 2014. Upper Pleistocene and Holocene palaeoenvironmental records in Cueva Mayor karst (Atapuerca, Spain) from different proxies: speleothem crystal fabrics, palynology, and archaeology. Int. J. Speleol. 43, 1–14.

Murray, A.S., Wintle, A., 2000. Luminescence dating of quartz using an improved single-aliquot regenerative-dose protocol. Radiat. Meas. 32, 57–73.

Navazo, M., Carbonell, E., 2014. Neanderthal settlement patterns during MIS 4–3 in Sierra de Atapuerca (Burgos, Spain). Quat. Int. 331, 267–277.

Navazo, M., Alonso-Alcalde, R., Benito-Calvo, A., Diez, J.C., Perez-Gonzalez, A., Carbonell, E., 2011. Hundidero: MIS 4 open air Neanderthal occupations in Sierra de Atapuerca. Archaeol. Ethnol. Anthropol. Eurasia 39, 29–41.

Ollé, A., Mosquera, M., Rodríguez, X.P., Lombera-Hermida, A., García-Antón, M.D., García-Medrano, P., Peña, L., Menéndez, L., Navazo, M., Terradillos, M., Bargalló, A., Márquez, B., Sala, R., Carbonell, E., 2013. The Early Middle Pleistocene technological record from Sierra de Atapuerca (Burgos, Spain). Quat. Int. 295, 138–167.

Ortega, A.I., 2009. Evolución geomorfológica del Karst de la Sierra de Atapuerca (Burgos) y su relación con los yacimientos pleistocenos que contiene. Ph.D. Dissertation. Universidad de Burgos.

Prescott, J.R., Hutton, J.T., 1994. Cosmic ray contributions to dose rates for luminescence and ESR dating: large depths and long-term time variations. Radiat. Meas. 23, 497–500.

Quam, R.M., Arsuaga, J.L., Bermúdez de Castro, J.M., Díez, C.J., Lorenzo, C., Carretero, J.M., García, N., Ortega, A.I., 2001. Human remains from Valdegoba cave (Huérmeces, Burgos, Spain). J. Hum. Evol. 41, 385–435.

Rodríguez, J., Burjachs, F., Cuenca-Bescós, G., García, N., Van der Made, J., Pérez-González, A., Blain, H.-A., Expósito, I., Lopez-García, J.M., García Antón, M., Allué, E., Cáceres, I., Huguet, R., Mosquera, M., Ollé, A., Rosell, J., Parés, J.M., Rodríguez, J.M., Díez, C., Rofes, J., Sala, R., Saladié, P., Vallverdú, J., Bennasar, M.L., Blasco, R., Bermúdez de Castro, J.M., Carbonell, E., 2011. One million years of cultural evolution in a stable environment at Atapuerca (Burgos, Spain). Quat. Sci. Rev. 30, 1396–1412.

Sánchez Yustos, P., Diez Martín, F., 2016. Dancing to the rhythms of the Pleistocene? Early Middle palaeolithic populations dynamics in NW iberia (Duero basin and cantabrian region). Quat. Sci. Rev. 121, 75–88.

Stevens, T., Buylaert, J.-P., Murray, A.S., 2009. Towards development of a broadly-applicable SAR TT-OSL dating protocol for quartz. Radiat. Meas. 44, 639–645.

Terradillos-Bernal, M., Díez Fernández-Lomana, C.J., Jordá-Pardo, J.-F., Benito-Calvo, A., Clemente, I., Marcos-Saiz, J.F., 2017. San Quirce (Palencia, Spain). A Neanderthal open air campsite with short term-occupation patterns. Quat. Int. 435, 115–128.

Tsukamoto, S., Duller, G.A.T., Wintle, A.G., 2008. Characteristics of thermally transferred optically stimulated luminescence (TT-OSL) in quartz and its potential for dating sediments. Radiat. Meas. 43, 1204–1218.

Wang, X.L., Wintle, A.G., Lu, Y.C., 2006. Thermally transferred luminescence in fine-grained quartz from Chinese loess: basic observations. Radiat. Meas. 41, 649–658.